Life Sciences 231 (2019) 116459

Contents lists available at ScienceDirect

Life Sciences

journal homepage: www.elsevier.com/locate/lifescie

Downregulation of LINC00460 decreases STC2 and promotes autophagy of head and neck squamous cell carcinoma by up-regulating microRNA-206

Kai Xue[a,1], Jinqiu Li[a,1], Shanji Nan[b], Xue Zhao[a], Chengbi Xu[a,*]

[a] Department of Otolaryngology-Head and Neck Surgery, the Second Hospital of Jilin University, Changchun 130041, PR China
[b] Department of Neurology, the Second Hospital of Jilin University, Changchun 130041, PR China

ARTICLE INFO

Keywords:
LINC00460
MicroRNA-206
STC2
Head and neck squamous cell carcinoma
Apoptosis
Autophagy

ABSTRACT

Aim: Head and neck squamous cell carcinoma (HNSCC) is one of the most prevalent types of cancer worldwide with unfavorable patient outcomes and relatively low survival rates. Long non-coding RNAs (lncRNAs) have been demonstrated to participate in the progression of HNSCC. The present study aimed to investigate the functional mechanism of lncRNA LINC00460 in HNSCC by mediating microRNA-206 (miR-206)/stanniocalcin-2 (STC2) axis.

Methods: The interactions among miR-206, LINC00460 and STC2 were identified, and the expression of LINC00460, miR-206 and STC2 in tissues and cells was determined. Gain- and loss-of function experiments were conducted to analyze effects of LINC00460, miR-206 and STC2 on the expression of apoptosis-related proteins, autophagy-related proteins, and the extents of AKT, ERK phosphorylation. Cell cycle distribution, apoptosis and the production of autophagosomes after transfection were evaluated to further explore the role of LINC00460/miR-206/STC2 axis in HNSCC.

Results: LINC00460 and STC2 were highly expressed while miR-206 was poorly expressed in HNSCC. Besides, miR-206 was found to bind to both LINC00460 and STC2. After the transfection of HNSCC cells with miR-206 mimic or si-LINC00460, the expression of STC2, AKT, ERK, as well as the extent of AKT, ERK phosphorylation all decreased, which facilitated the apoptosis and autophagy of HNSCC cells.

Conclusion: Collectively, the apoptosis and autophagy of HNSCC can be facilitated by downregulating LINC00460, which highlights a novel target in the treatment of HNSCC.

1. Introduction

Head and neck squamous cell carcinoma (HNSCC), which includes tumors of the oral cavity, larynx and oroparynx, has been the six most prevalent type of cancer worldwide and the most recurrent malignancy of the upper aerodigestive tract [1,2]. The incidence of HNSCC has increased with an estimated occurrence rate of nearly 135.1 per 100,000 in China yearly [3]. HNSCC is characterized as a solid tumor with highly aggressive phenotypes and inferior clinical results mainly due to the local tumor recurrence, regional and distant lymph node metastasis [4]. Irrespective of the great advancements made in the treatment of HNSCC with the application of chemotherapy, radiotherapy and surgery in the past decades, moderate improvements have improved the five-year survival rates of HNSCC patients [5]. Therefore, it is necessary to further develop biomarkers and therapeutic targets for HNSCC. Eminently, the importance of long noncoding RNAs (lncRNAs) has been reported to be vital for the development of cancer [6], and lncRNA LINC00460 served as a new and valuable prognostic biomarker for the diagnosis and treatment of esophageal squamous cell carcinoma (ESCC) [7].

LncRNA, a kind of non-coding RNA longer than 200 nt, are essential for the regulation of various biological processes, the abnormal expressions of which have been detected in many disease types, especially in cancers [4]. It has become increasingly significant to understand the roles of lncRNAs in different diseases so as to identify potential lncRNAs for disease diagnosis, treatment and prognosis [8]. LINC00460, abbreviation of a novel identified lncRNA named long intergenic non-protein coding RNA 460, is located specifically in the chromosome 13q33.2 region and has a length of 935 bp [9]. It was discovered that the expression of LINC00460 in ESCC tissues was high and it was

* Corresponding author at: Department of Otolaryngology-Head and Neck Surgery, the Second Hospital of Jilin University, No. 218, Ziqiang Street, Nanguan District, Changchun 130041, Jilin Province, PR China.
E-mail address: chengbix@126.com (C. Xu).
[1] These authors contributed equally to this work.

https://doi.org/10.1016/j.lfs.2019.05.015
Received 24 January 2019; Received in revised form 5 May 2019; Accepted 7 May 2019
Available online 08 May 2019

closely related to tumor node metastasis (TNM) stage and lymph node metastasis [7]. However, the expression and biological function of LINC00460 in HNSCC tissues and cells have not been reported yet. In this present study, various online websites predicted the existence of multiple binding sites between LINC00460 and microRNA-206 (miR-206) as well as miR-206 and STC2. MiR-206, which belongs to the vast family of miRNAs, has been discovered to regulate several fundamental processes such as cellular proliferation, differentiation and apoptosis [10]. Even some kinds of miRNAs (let-7d and miR-205) have been identified as possible diagnostic and prognostic biomarkers for cancer [1], while few studies have researched miR-206 expression in HNSCC to the best of our knowledge. STC2, a member of the stanniocalcin family, is a homologue for a glycoprotein hormone [11]. A study has shown that STC2 is upregulated in human colorectal cancer and prostate cancer, but the precise role of STC2 in HNSCC still remains unexplored [2,12,13]. With the aforementioned evidence as basis, we hypothesized that the promotion of apoptosis and autophagy of HNSCC can be facilitated by silencing LINC00460 and the underlying molecular mechanisms in relation to miR-206-mediated STC2 inhibition.

2. Materials and methods

2.1. Ethics statement

This study was performed with approval of the Medical Ethics Committees of the Second Hospital of Jilin University. All patients or their parents or guardians provided informed consent prior to their participation.

2.2. Microarray-based gene analysis

The Cancer Genome Atlas (TCGA) (http://cancergenome.nih.gov/) database was used to retrieve gene expression data of HNSCC, and statistical analysis was conducted using the R software. The edge R package in the R software was employed for performing a differential analysis of the transcriptome profiling data [14]. False positive discovery (FDR) correction was employed on the *p*-value with package multitest. Besides, the differentially expressed genes (DEGs) were screened in accordance to the screening criteria of FDR < 0.05 and $|\log2 \text{ (fold change)}| > 2$. Informative websites such as microRNA (http://34.236.212.39/microrna/getMirnaForm.do), Targetscan.org (http://www.targetscan.org/vert_71/), Starbase (http://starbase.sysu.edu.cn/browseClipSeq.php) and miRSearch V3.0 (https://www.exiqon.com/miRSearch) were used for predicting the targeted miRNA of the target genes.

2.3. Study subjects

Fifty-four HNSCC tissues and their adjacent normal tissues were resected from HNSCC patients with complete pathological information from March 2016 to August 2017 in the Second Hospital of Jilin University. The adjacent normal tissues without tumor cell infiltration were selected as controls. The resected HNSCC samples were the primary lesion without any tumor history, family medical history of the HNSCC, or any exceptional treatments before. The relevant clinicopathological data, including the patients' age, gender, tumor location, T stage and differentiation degree of HNSCC patients were analyzed. The correlation analysis was conducted between the clinicopathological features of HNSCC and the expression of LINC00460, miR-206 and STC2.

Fresh HNSCC tissues and their adjacent normal tissues were washed repeatedly in normal saline, sliced into sections with a volume of 1.0 cm × 1.0 cm × 0.5 cm and fixed with 10% formaldehyde immediately.

Table 1
The primer sequences for RT-qPCR.

Gene	Sequence
miR-206	F: 5′-CAGATCCGATTGGAATGTAAGG-3′ R: 5′-TATGCTTGTTCTCGTCTCTGTGTC-3′
LINC00460	F: 5′-ACAGCATGAGCCAGGACATC-3′ R :5′-GAAAGCTGCAACATGCTCCC-3′
STC2	F: 5′-GCGTGCAGGTTCAGTGTGA-3′ R: 5′-GGCCAGTCTCCCTACTGCT-3′
ERK	F: 5′-TACACCAACCTCTCGTACATCG-3′ R: 5′-CATGTCTGAAGCGCAGTAAGATT-3′
AKT	F: 5′-GTCATCGAACGCACCTTCCAT-3′ R: 5′-AGCTTCAGGTACTCAAACTCGT-3′
GAPDH	F: 5′-GGAGCGAGATCCCTCCAAAAT-3′ R: 5′-GGCTGTTGTCATACTTCTCATGG-3′
U6	F: 5′-CTTCGGCAGCACATATACTAAAAT-3′ R: 5′-CGCTTCACGAATTTGCGTGTCAT-3′

Note: F, forward; R, reverse; RT-qPCR, reverse transcription quantitative polymerase chain reaction; GAPDH, glyceraldehyde phosphate dehydrogenase; miR-206, microRNA-206; STC2, Stanniocalcin-2; AKT, Protein kinase B.

2.4. Reverse transcription quantitative polymerase chain reaction (RT-qPCR)

Total RNA was extracted from the tissues and cells in accordance with the instructions of the Trizol (Invitrogen Co, Ltd., Carlsbad, California, USA) reagent. The designed primers listed in Table 1 were synthesized by the Aoke Biotechnology Company (Jiangsu, China). Complementary DNA (cDNA) was synthesized in the 25 μL PCR reaction system according to the instructions of the All-in-one and First-Strand cDNA synthesis kits (Genecopoeia Company, CA, USA). U6 was selected as the internal reference for miR-206, while glyceraldehyde-3-phosphate dehydrogenase (GAPDH) served as an internal reference for AKT and ERK. The PCR reaction conditions were as follows: pre-denaturation at 95 °C for 10 min, 40 cycles of denaturation at 94 °C for 30 s, annealing at 59 °C for 30 s, and extension at 72 °C for 30 s. Each sample was tested three times to obtain the mean value. The $2^{-\Delta Ct}$ method was employed to calculate the relative expression of genes, in which $\triangle CT = CT_{\text{(target gene)}} - CT_{\text{(internal reference)}}$.

2.5. Fluorescence in situ hybridization (FISH) technique

The HNSCC tissues were added with 0.5 mg/mL collagenase (50 mL), and then filtrated after 30 min of oscillation and detachment at 37 °C, followed by gradient centrifugation with the 8.2% broad-spectrum separating medium (nycodenz, Shanjin Biotechnology Co., Ltd., Shanghai, China), suspended and cultivated in a fluorescent chamber. Subsequently, basal medium (500 μL) was added to each well. The cells were washed with phosphate buffer saline (PBS) 3 times, 2 min each. Then the cells were fixed in 4% paraformaldehyde/0.1 MPB fixation solution containing 1/1000 diethy pyrocarbonate (DEPC) at room temperature for 20–30 min. A combination of 30% H_2O_2 and pure methanol in the ratio of 1:50 was prepared and then treated for 30 min at room temperature. Afterwards, the cells were washed with distilled water 3 times and then treated according to the instructions of the RNA-FISH kits (BOSTER Biological Technology Co., Ltd., Wuhan, China). The cellular sublocalization of LINC00460 was observed under a fluorescence microscope (Olympus, Tokyo, Japan).

2.6. RNA pull-down assay

Initially, 50 nM biotin labeled WT-bio-miR-206 and MUT-bio-miR-206 were transfected into cells. After 48 h, the cells were collected and lysed with specific lysis buffer (Ambion, Austin, TX, USA) for 10 min. The lysates were cultured with M-280 streptavidin magnetic beads (S3762, Sigma-Aldrich Chemical Company, St Louis, MO, USA) pre-

coated with RNase-free BSA and yeast tRNA (TRNABAK-RO, Sigma-Aldrich Chemical Company, St Louis, MO, USA) at 4 °C for 3 h. The beads were washed 8 times and incubated with protease K buffer at 55 °C for 30 min. Then the supernatant was transferred to a new centrifugal. The combined RNA was purified by Trizol and the lincRNA00460 enrichment was assessed by RT-qPCR.

2.7. Dual luciferase reporter gene assay

The biological prediction website microRNA.org and the RNA 22 website were employed to analyze the target genes of miR-206, and the dual luciferase reporter gene assay was further used to verify whether STC2 and LINC00460 were direct targets of miR-206. The binding sequences of STC2 and LINC00460 were predicted to be regulated by miR-206. The wild type (Wt) sequences of STC2–3'UTR, LINC00460–3'UTR and their mutant (Mut) ones were designed and synthesized, and cloned into the pmir GLO vector respectively. Four distinctively constructed plasmids namely, pmir GLO-Wt-STC2, pmir GLO-Wt-LINC00460, pmir GLO-Mut-STC2 and pmir GLO-Mut-LINC00460, were obtained. The transfection reagent lipofectamine™ 2000 (Invitrogen Co., Ltd., Carlsbad, California, USA) was used to co-transfect four recombinant vector plasmids with miR-206 mimic or negative control (NC) respectively into the human embryonic kidney cells HEK-293 T (Cells Resource Center, Shanghai life Science Research Institute, Academy of Science, Shanghai, China). The cells were collected and lysed after transfection for 48 h. The Dual-Luciferase Reporter Gene Assay System kit (Promega Corporation, Madison, MI, USA) was employed so as to test the luciferase activity on the Luminometer TD-20/20 (E5311, Promega Corporation, Madison, MI, USA). Each experiment was repeated three times.

2.8. Cell culture and screening

The following cell lines were purchased from Cells Resource Center, Shanghai life Science Research Institute, Academy of Science (Shanghai, China): oral cavity squamous cell carcinoma cell line PCI-13 [15], hypopharyngeal squamous cell carcinoma cell line FaDu [16,17], the tongue squamous cell carcinoma cell line SCC-15 [16,17], the laryngeal squamous cell carcinoma cell line UM-SCC-10A [16,18]. Cell lines were cultured in BPMI 1640 medium (HyClone Laboratories Inc., Nebraska, USA) (containing 10% calf serum, 1 U/mL penicillin and 2.5 μg/mL amphotericin) containing 10% fetal bovine serum (FBS), and cultured in an sterile incubator (Thermo Fisher Scientific, Inc., Waltham, MA, USA) with saturated humidity at 37 °C with 5% CO_2 for 24 h. Cell morphology and density as well as bacterial infestation were observed. After incubation for 48–72 h, the culture medium was renewed or passaged. The total RNA from the aforementioned 4 cell lines was extracted in accordance with the Trizol kits (Invitrogen Company, Carlsbad, California, USA), and the expression of LINC00460 in these 4 cell lines was detected by RT-qPCR, so as to screen the cell lines with the highest LINC00460 expression for subsequent experiments.

2.9. Cell transfection

HNSCC cells were introduced with a series of miR-206 mimic, miR-206 inhibitor, siRNA targeting LINC00460 (si-LINC00460), and vector overexpressing LINC00460 (LINC00460 vector) or NC plasmid. Before transfection, the HNSCC cells were inoculated into 8-well plates. Upon attaining a cell density of 30–50%, the cells were transfected in accordance to the instructions of lipofectamine 2000 (Invitrogen, Carlsbad, CA, USA). The 250 μL serum-free Opti-MEM medium (Gibco, Grand Island, N.Y., USA) was used to dilute 100 pmol plasmid to a final concentration of 50 nM and 5 μL lipofectamine 2000, respectively. The above two diluted solutions were incubated together with cells under conditions of 5% CO_2 at room temperature for 6–8 h. After that, the mixture was cultured with complete medium for 24–48 h for subsequent experiments.

2.10. Western blot analysis

HNSCC cells were lysed with precooled cell lysis buffer (containing 1% protease inhibitor) on ice in an attempt to extract protein, and the protein concentration was detected using the bicinchoninic acid (BCA) assay. A total of 50 μg protein was separated with 10% sodium dodecyl sulfate polyacrylamide gel electrophoresis (SDS-PAGE). The separated proteins were transferred onto a polyvinylidene fluoride (PVDF) membrane through the semi-dry transfer method. The PVDF membrane was blocked using 5% skimmed milk and rinsed using the Tris-buffered saline (TBS) buffer 3 times, 10 min each. The membrane was incubated at 4 °C overnight with the following diluted (1: 1000) primary rabbit anti mouse polyclonal antibodies: STC2 (ab63057), AKT (ab8805), ERK (ab54230), p-AKT (ab38449), p-ERK (ab214362), LC3B (ab51520), Beclin 1 (1:2000), (ab62557), cleaved-PARP (ab32064), Bax (ab32503), and cleaved-caspase 3 (ab2302). All these antibodies were purchased from Abcam (Cambridge, UK). The next day, after a thorough rinse with Tris-buffered saline with Tween 20 (TBST), the membrane was incubated using a combination of secondary antibody conjugated with horseradish peroxidase (HRP) (1: 5000) for 2 h. The enhanced chemiluminescent (ECL) reagent was used for developing. GAPDH served as the internal reference, and the ratio of the gray value of the target band to the gray value of the internal reference band was depicted as the relative expression of protein. The experimental result was the average of three repetitions.

2.11. Flow cytometry

The propidium iodide (PI) staining was performed for cell cycle detection. According to the instructions of the cell cycle detection kit (Beyotime Biotechnology Company, Shanghai, China), after 48 h of cell transfection, the cells were fixed with 5 mL 70% (pre-cooled) ethanol at 4 °C overnight. After centrifugation, the cells were resuspended using PBS, and gently triturated into a cell suspension. Approximately 3 μL RNase-A was added to attain a final concentration of 50 μg/mL. Afterwards, the cells were bathed and detached at 37 °C for 30 min. About 50 μL PI was added until the final concentration was about 65 μg/mL, and then the cells were stained in ice bathe in conditions devoid of light for 30 min.

Annexin V-FITC/PI double staining was applied for cell apoptosis detection. According to the instructions of the apoptosis detection kits (BestBio Co., Ltd., Shanghai, China), HNSCC cells in the logarithmic growth stage were washed with PBS two times, suspended with 400 μL 1 × Binding Buffer at a concentration of approximately 1×10^6 cells/mL. The cell suspension was added with 5 μL Annexin V-FITC and incubated for 15 min. After the addition of 10 μL PI, the cells were incubated for 15 min. Cells were filtered using a 300-mesh (aperture: 40–50 μm) nylon net. Cell cycle and apoptosis were detected using a FACS Calibur flow cytometer (BD Biosciences, San Diego, CA, USA) at a wavelength of 488 nm.

2.12. Immunofluorescence assay

The cells were fixed with 4% paraformaldehyde for 20 min, and washed with PBS three times. Next, the cells were permeabilized with 0.5% trixon X-100 for 5 min, then repeatedly washed with PBS three times, and incubated in 5% bovine serum albumin (BSA) for 1 h to prevent non-specific staining. The cells were incubated with primary antibodies diluted with the blocking serum (1: 200) at 4 °C overnight, washed with precooled PBS three times. The cells were then incubated with the FITC-labeled secondary antibody diluted with blocking serum (1: 200) at 37 °C for 2 h, and then washed with PBS three times. The nucleus was stained with 10% 4′,6-diamidino-2-phenylindole (DAPI) for 5 min. The cells were mounted with the fluorescence anti-quenching

agent. Results of DAPI staining (blue) and FITC labeling immunofluorescence (green) were observed under an inverted fluorescence microscope (NIKON Corporation, Japan). Upon occurrence of autophagy, a lot of aggregations of autophagosomes presenting green fluorescent spots in the cytoplasm were observable, especially near the nucleus.

2.13. Statistical analysis

Statistical analysis was conducted using the SPSS 21.0 statistical software (IBM Corp. Armonk, NY, USA). Measurement data were presented as mean ± standard deviation. Independent sample *t*-test was used for comparison between two groups, paired *t*-test was applied for comparison within groups, and one-way analysis of variance (ANOVA) was employed for comparing among multiple groups. A value of $p < 0.05$ was considered to be statistically significant.

3. Results

3.1. LINC00460 and STC2 are upregulated while miR-206 is downregulated in HNSCC

The data from the TCGA database showed that STC2 was highly expressed in HNSCC (Fig. 1A) and was associated with the prognosis of HNSCC (Fig. 1B). Using four websites (microRNA, Targetscan.org, Starbase and miRSearch V3.0), the binding sites among miR-24, miR-206, and STC2 were predicted (Fig. 1C), among which only miR-206 was found to be poorly expressed in HNSCC based on the data in the TCGA database (Fig. 1D). Finally, the existence of a binding site between LINC00460 and miR-206 was confirmed from the RNA22 website, and expression of LINC00460 was highly expressed in HNSCC (Fig. 1E). The expression of LINC00460, miR-206 and mRNA expression of STC2 in the HNSCC and its adjacent normal tissues were determined by RT-qPCR. In comparison with the adjacent normal tissues, the expression of LINC00460, and the mRNA expression of STC2 in the HNSCC tissues were significantly upregulated, while that of miR-206 was significantly downregulated (all $p < 0.05$) (Fig. 1F). It could be concluded that miR-206 was poorly expressed while LINC00460 and STC2 were highly expressed in HNSCC.

3.2. Expression of LINC00460, miR-206 and STC2 is closely related to the progression of HNSCC

The associations between the expression of LINC00460, miR-206 and STC2 in 54 patients with HNSCC and the clinicopathological features were analyzed. It was found that the expression of LINC00460, miR-206 and STC2 was not related to any parameters like the age, gender and tumor location (all $p > 0.05$) but was closely related to the TNM stage and differentiation degree of HNSCC (both $p < 0.05$; Table 2).

3.3. LINC00460 is located in the cytoplasm

The RNA-FISH analysis was employed in order to analyze the location of LINC00460 in cells. The results (Fig. 2) showed that LINC00460 was mainly expressed and localized in the cytoplasm of HNSCC cells, and that the expression of LINC00460 in the cytoplasm was higher than the expression observed in the nucleus. This suggested that LINC00460 might function primarily in the cytoplasm.

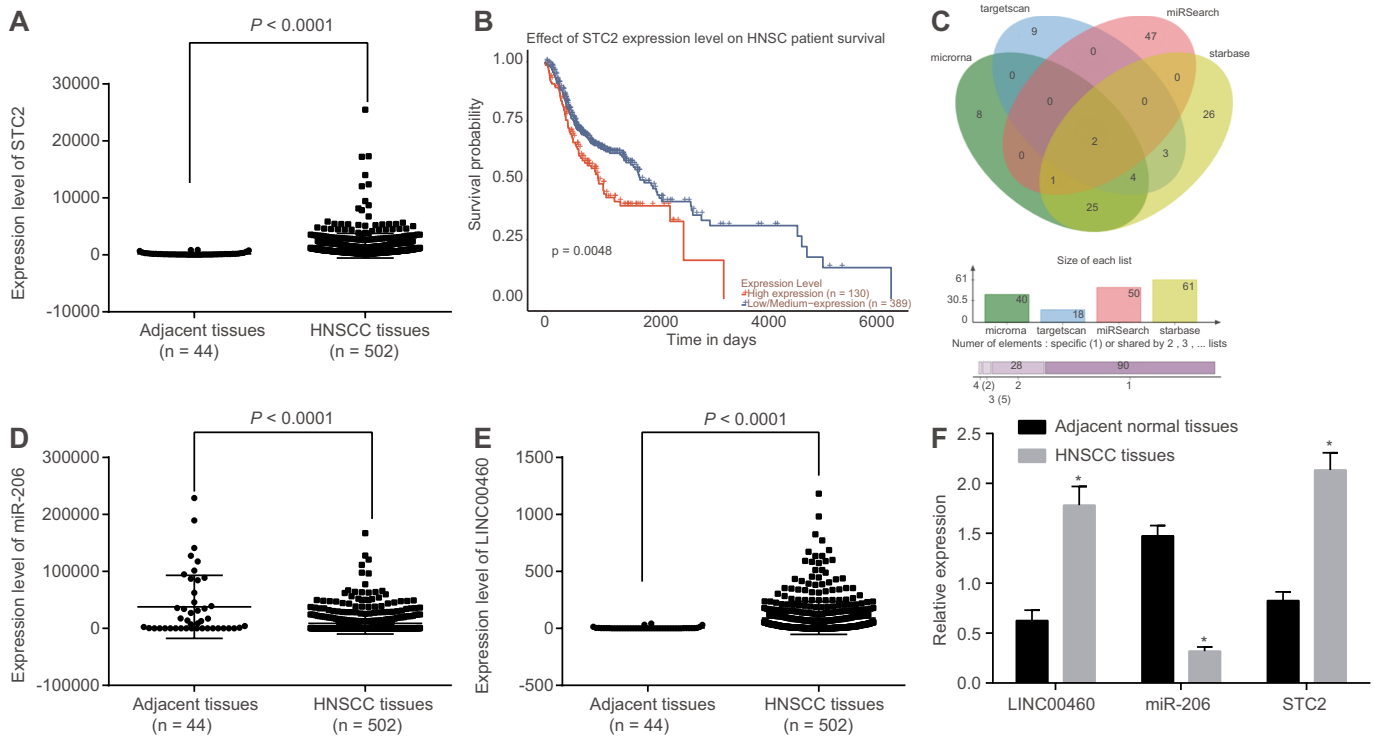

Fig. 1. LINC00460 and STC2 are highly expressed while miR-206 is poorly expressed in HNSCC tissues. A, expression of STC2 in HNSCC tissues and adjacent tissues as shown in the TCGA database. B, the survival data of patients with high and low STC2 expressions as shown in TCGA database. C, miRNA that targeted STC2 as predicted in four online databases. D, expression of miR-206 in HNSCC tissues and adjacent normal tissues as per the TCGA database. E. expression of LINC00460 in HNSCC tissues and adjacent normal tissues in the TCGA database. F, expression of LINC00460, miR-206 and STC2 in HNSCC tissues and adjacent normal tissues determined by RT-qPCR. * $p < 0.05$ *vs.* adjacent normal tissues. All data in RT-qPCR were measurement data and expressed as mean ± standard deviation and analyzed using *t*-test. The experiment was repeated 3 times. STC2, Stanniocalcin-2; miR-206, microRNA-206; HNSCC, head and neck squamous cell carcinoma; TCGA, The Cancer Genome Atlas; RT-qPCR, reverse transcription quantitative polymerase chain reaction.

Table 2
Correlation analysis of clinicopathological features of HNSCC with expression of LINC00460, miR-206 and STC2.

Clinicopathological features	Case	LINC00460	*p*	miR-206	*p*	STC2	*p*
Age (years)							
< 60	42	1.457 ± 0.311	0.984	0.253 ± 0.076	0.780	1.755 ± 0.331	0.310
≥60	12	1.455 ± 0.236		0.246 ± 0.077		1.866 ± 0.329	
Gender							
Male	30	1.484 ± 0.366	0.454	0.263 ± 0.094	0.212	1.800 ± 0.397	0.616
Female	24	1.423 ± 0.169		0.237 ± 0.040		1.754 ± 0.228	
Differentiation degree							
Low and medium differentiation	30	1.373 ± 0.192	0.018*	0.229 ± 0.064	0.014*	1.692 ± 0.306	0.027*
High differentiation	24	1.562 ± 0.364		0.279 ± 0.081		1.890 ± 0.333	
TNM stage							
I-II	21	1.578 ± 0.373	0.003*	0.293 ± 0.076	0.001*	1.902 ± 0.298	0.029*
III a	33	1.380 ± 0.201		0.225 ± 0.063		1.702 ± 0.331	
Location							
Nasal cavity	16	1.510 ± 0.377	0.842	0.292 ± 0.082	0.061	1.820 ± 0.273	0.686
Tongue	14	1.455 ± 0.364		0.231 ± 0.098		1.778 ± 0.514	
Gum	11	1.430 ± 0.147		0.224 ± 0.039		1.752 ± 0.267	
Throat	13	1.416 ± 0.191		0.247 ± 0.039		1.755 ± 0.202	

Note: *, $p < 0.05$ compared with non-pathological factors; TNM, tumor, nodes, metastasis; STC2, stanniocalcin-2; miR-206, microRNA-206; HNSCC, head and neck squamous cell carcinoma.

3.4. LINC00460 and STC2 could bind to miR-206

The target genes of miR-206 were analyzed using the biological prediction websites microRNA.org and RNA22, and the miR-206 binding sites were identified on STC2 3'UTR and LINC00460 (Fig. 3A, B). The results of dual luciferase reporter gene assay showed that the transfection of miR-206 mimic led to a significantly decreased luciferase activity of both WT-LINC00460 and WT-STC2 (both $p < 0.05$) (Fig. 3C, D). RNA pull-down assay showed that WT-bio-miR-206 binds more to LINC00460 than MUT -bio-miR-206 and NC. (both $p < 0.05$; Fig. 3E). These findings provided evidence supporting that miR-206 specifically inhibited STC2 and LINC00460 and miR-206 could be sponged by LINC00460.

3.5. INC00460 is highly expressed in PCI-13 cell line

RT-qPCR was used to detect the expression of LINC00460 in PCI-13, FaDu, SCC-15 and UM-SCC-10A cell lines. The results (Fig. 4) showed that LINC00460 was expressed in the above-mentioned cell lines. LINC00460 expression in the PCI-13 cell line was higher than the expression in the FaDu, SCC-15 and UM-SCC-10A cell lines (all $p < 0.05$). Therefore, PCI-13 cell line was selected for the subsequent experiments.

3.6. Over-expressed miR-206 or silenced LINC00460 downregulates mRNA and protein expression of STC2, and inhibits the AKT signaling pathway

RT-qPCR and western blot analysis were used to measure the expression of LINC00460, miR-206, STC2, AKT, ERK, as well as the extent of AKT and ERK phosphorylation, and the results are shown in Fig. 5. On comparing with the blank group and the NC group, it was observed that the LINC00460 expression had decreased in the si-LINC00460 group while it had increased in the LINC00460 vector group ($p < 0.05$). In comparison with the miR-206 mimic + NC group, LINC00460 expression was significantly elevated in the LINC00460 vector + miR-206 mimic group, while the si-LINC00460 + miR-206 inhibitor group showed a reduced LINC00460 expression in contrast to the miR-206 inhibitor + NC group (Fig. 5A; $p < 0.05$). In contrast to the blank and NC groups, the miR-206 expression was higher in the miR-206 mimic group while it was lower in the miR-206 inhibitor group. In comparison with the LINC00460 vector + mimic NC group, the LINC00460 vector + miR-206 mimic group exhibited a significantly elevated miR-206 expression, while the si-LINC00460 + miR-206 inhibitor group presented with an obviously reduced miR-206 expression compared with the si-LINC00460 + inhibitor NC group (Fig. 5B; $p < 0.05$). The mRNA and protein expression of STC2, AKT and ERK, as well as the extent of AKT and ERK phosphorylation was further examined, and the results (Fig. 5C, D) showed that compared with the blank and NC groups, the expression of STC2, AKT and ERK, as well as the extent of AKT and ERK phosphorylation was significantly decreased in the miR-206 mimic group and the si-LINC00460 group in contrast to the blank group and the NC group (all $p < 0.05$), while the expression of STC2, AKT and ERK, as well as the extent of AKT and ERK phosphorylation had significantly increased in the miR-206 inhibitor group and the LINC00460 vector group (all $p < 0.05$). No evident difference was observed in terms of the expression of miR-206, STC2, AKT and ERK, as well as the extent of AKT and ERK phosphorylation among the si-LINC00460 + miR-206 inhibitor group and the LINC00460 vector + miR-206 mimic group (all $p > 0.05$). The above results showed that an upregulated miR-206 or downregulated LINC00460 correspondingly downregulates STC2, and blocks activation of the AKT signaling pathway.

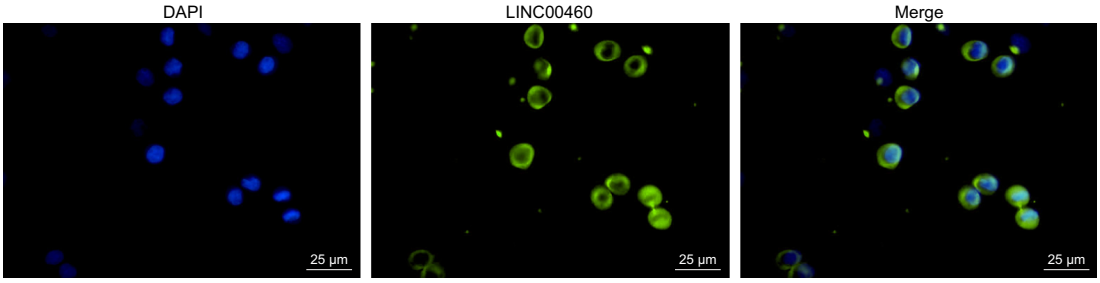

Fig. 2. Based on the results of RNA-FISH, LINC00460 is located in the cytoplasm (400 ×). FISH, fluorescence *in situ* hybridization.

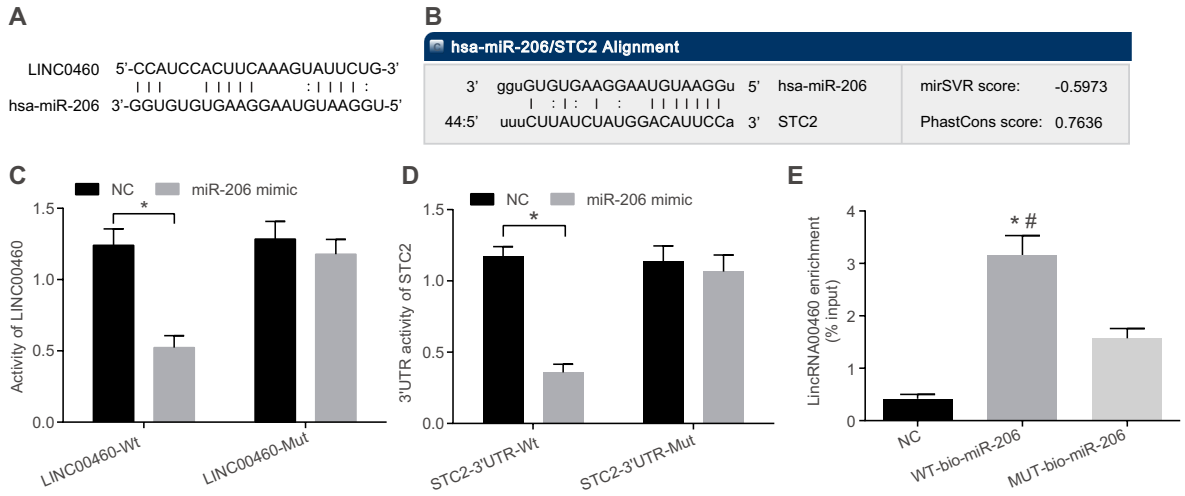

Fig. 3. STC2 and LINC00460 are verified to be bound by miR-206. A, the predicted binding site of LINC00460 and miR-206. B, the predicted binding site of miR-206 on 3'UTR of STC2. C-D, the luciferase activity of LINC00460-Wt/Mut and STC2-Wt/Mut detected by dual luciferase reporter gene assay; * $p < 0.05$ *vs.* the NC group. E, enrichment of miR-206 by LINC00460; * $p < 0.05$ vs. the NC group; # $p < 0.05$ vs.MUT-bio-miR-206. Results of luciferase activity and RNA pull-down assay were measurement data, expressed by mean ± standard deviation and analyzed using *t*-test. The experiment was repeated three times. STC2, Stanniocalcin-2; miR-206, microRNA-206; UTR, untranslated region; Wt, wild type; Mut, mutant type; NC, negative control.

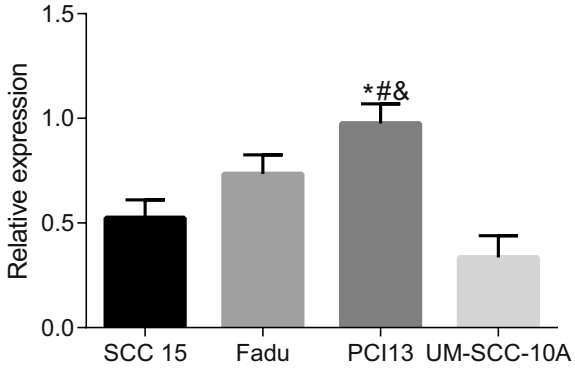

Fig. 4. LINC00460 is expressed at the highest level in PCI-13 cell line among the four kinds of HNSCC cell lines. * $p < 0.05$ *vs.* SCC-15 cell line, # $p < 0.05$ *vs.* FaDu cell line, & $p < 0.05$ *vs.* UM-SCC-10A cell line. Data of RT-qPCR were measurement data, expressed by mean ± standard deviation and analyzed using one-way ANOVA, and the experiment was repeated three times. HNSCC, head and neck squamous cell carcinoma; RT-qPCR, reverse transcription quantitative polymerase chain reaction; ANOVA, analysis of variance.

3.7. LINC00460 silencing affects cell cycle distribution and promotes apoptosis in HNSCC cells by sponging miR-206

PI staining and Annexin V/PI double staining detection were performed in an attempt to detect the cell cycle distribution and apoptosis of HNSCC cells, and the results showed that (Fig. 6) the apoptosis rates of cells in the blank group, the NC group, the miR-206 mimic group, the miR-206 inhibitor group, the si-LINC00460 group, the LINC00460 vector group, the si-LINC00460 + miR-206 inhibitor group and the LINC00460 vector + miR-206 mimic group were: (7.04 ± 0.42)%, (6.75 ± 0.35)%, (12.13 ± 1.072)%, (4.47 ± 0.25)%, (10.95 ± 0.87)%, (4.83 ± 0.29)%, (7.01 ± 0.39)%, and (6.56 ± 0.51)%, respectively. In comparison with the blank group and the NC group, cells in the miR-206 mimic group and the si-LINC00460 group presented with a higher number of cells arrested in the G0/G1 phase with a smaller proportion in the S phase, with a significantly elevated apoptosis rate (all $p < 0.05$). The miR-206 inhibitor group and the LINC00460 vector group has less cells arrested in the G0/G1 phase than the S phase, with a significantly decreased apoptosis rate than the rate observed in the blank group and the NC group (all $p < 0.05$). Both cell cycle and the apoptosis rate of the si-LINC00460 + miR-206 inhibitor group and the LINC00460 vector + miR-206 mimic group showed no prominent change (all $p > 0.05$). The results showed that the upregulation of miR-206 or silencing of LINC00460 could arrest the HNSCC cells in the G0/G1 stage, hinder cell cycle transformation from G1 stage to S stage and increase cell apoptosis rate.

3.8. Over-expression of miR-206 or silencing of LINC00460 promotes apoptosis of HNSCC cells

The western blot analysis was employed for analysis of the impact of over-expressed miR-206 or silenced LINC00460 on the apoptosis of HNSCC cells by measuring the expression of apoptosis-related proteins, and the results (Fig. 7) indicated that the difference between the blank group and the NC group was not statistically significant ($p > 0.05$). In comparison with the blank group and the NC group, the protein expression of cleaved-PARP, Bax and cleaved-caspase 3 in both the miR-206 mimic group and the si-LINC00460 group had markedly increased (all $p < 0.05$). The expression of cleaved-PARP, Bax and cleaved caspase-3 in the miR-206 inhibitor group and the LINC00460 vector group had significantly declined in comparison to the blank group and the NC group (all $p < 0.05$). No significant difference was evident in the protein expression of cleaved-PARP, Bax and cleaved caspase-3 between the si-LINC00460 + miR-206 inhibitor group and the LINC00460 vector + miR-206 mimic group upon comparison (all $p > 0.05$). The above results show that the over-expression of miR-206 or silencing of LINC00460 could promote the apoptosis of HNSCC cells.

3.9. Over-expression of miR-206 or silencing of LINC00460 enhances autophagy of HNSCC cells

Immunofluorescence assay and western blot analysis were used to detect the impact of over-expressed miR-206 or silencing LINC00460 on the autophagy of HNSCC cells through detection of the autophagosomes and autophagy-related proteins, and the results (Fig. 8) are evident of no statistically significant difference between the blank group and the NC group ($p > 0.05$). In comparison with the blank group and the NC group, the miR-206 mimic group and the si-LINC00460 group showed an increased number of autophagosomes, with increased granular green fluorescence predominantly around the nucleus under microscopic evaluation, along with an increased ratio of LC3 II/LC3 I and expression of Beclin 1 (all $p < 0.05$). In the miR-206 inhibitor group and the

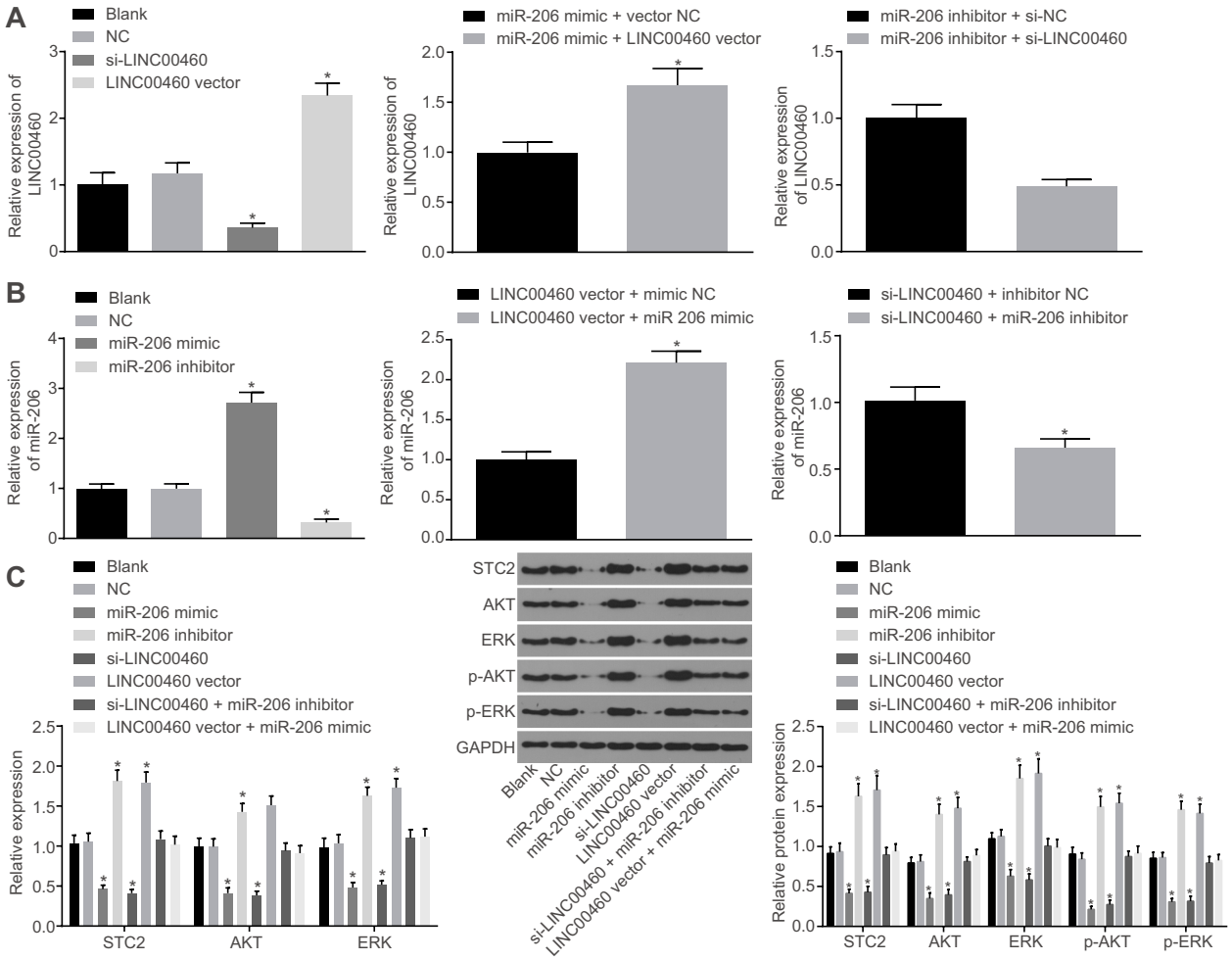

Fig. 5. The mRNA and protein expression of STC2, AKT, ERK as well as the extent of AKT and ERK phosphorylation are decreased by the high expression of miR-206 or low expression of LINC00460. A-B, the expression of miR-206 and LINC00460 in cells after transfection with si-LINC00460, LINC00460 vector, miR-206 mimic and miR-206 inhibitor examined by RT-qPCR. C, the mRNA expression of STC2, AKT and ERK in cells after transfection with si-LINC00460, LINC00460 vector, miR-206 mimic and miR-206 inhibitor determined by RT-qPCR. D, the protein expression of STC2, AKT, ERK as well as the extent of AKT and ERK phosphorylation in cells after transfection with si-LINC00460, LINC00460 vector, miR-206 mimic and miR-206 inhibitor. * $p < 0.05$. Data of RT-qPCR and western blot analysis were measurement data, expressed by mean ± standard deviation and analyzed using one-way ANOVA, and the experiment was repeated three times. STC2, Stanniocalcin-2; miR-206, microRNA-206; AKT, Protein kinase B; RT-qPCR, reverse transcription quantitative polymerase chain reaction; ANOVA, analysis of variance.

LINC00460 vector group, the number of autophagosome was obviously reduced, the ratio of LC3 II/LC3 I and expression of Beclin 1 decreased markedly, and the overall autophagy was restrained as compared to the blank group and the NC group (all $p < 0.05$). No significant changes were observed in the number of autophagosome and the ratio of LC3 II/LC3 I and expression of Beclin 1 between the si-LINC00460 + miR-206 inhibitor group and the LINC00460 vector + miR-206 mimic group ($p > 0.05$). Therefore, it could be concluded that over-expression of miR-206 or silencing of LINC00460 could stimulate the autophagy of HNSCC cells.

4. Discussion

HNSCC, the sixth most common non-skin cancer worldwide, has been acknowledged as a morbid and customarily deadly disease with a total incidence of 600,000 cases each year and mortality rate of 50% [19]. LncRNAs have been extensively demonstrated to be of vital functionality in cancer development, by means of key regulators in gene regulation and a broad range of biological processes, and lncRNAs also act as a molecular sponge to silence miRNA expression [4]. A novel lncRNA named LINC00460 was evidently over-expressed in a majority of tumor tissues and ESCC cell lines, thus indicating its use as an oncogene and a valuable biomarker for ESCC diagnosis and treatment [7]. However, the precise functional mechanisms of LINC00460 in HNSCC have remained poorly researched. Therefore, this study was performed with the aim of assessing the importance of LINC00460/STC2/miR-206 axis in the apoptosis and autophagy of HNSCC. Consequently, through sequential experimentation, this study demonstrated that down-regulation of LINC00460 could downregulate STC2 *via* miR-206, thus facilitating HNSCC cell apoptosis and autophagy.

Initially, our experimental results showed that LINC00460 and STC2 were highly expressed, while miR-206 was poorly expressed in HNSCC. Consistent with our study, Liang et al. found that LINC00460 was over-expressed in a majority of tumor tissues, including nasopharyngeal carcinoma (NPC), one of the most common forms of head and neck tumors, and was relatively greater than that in normal tissues [7,20]. There was also statistical evidence showing that the low levels of certain kinds of miRNAs were closely related with disease recurrence rate and severity at diagnosis and treatment [1]. For example, Zheng et al. suggested that miR-206 was significantly decreased in LSCC than in adjacent normal tissues [21]. In addition, Yoshiaki Kita and his team suggested that the patients with a higher STC2 expression in the tumors

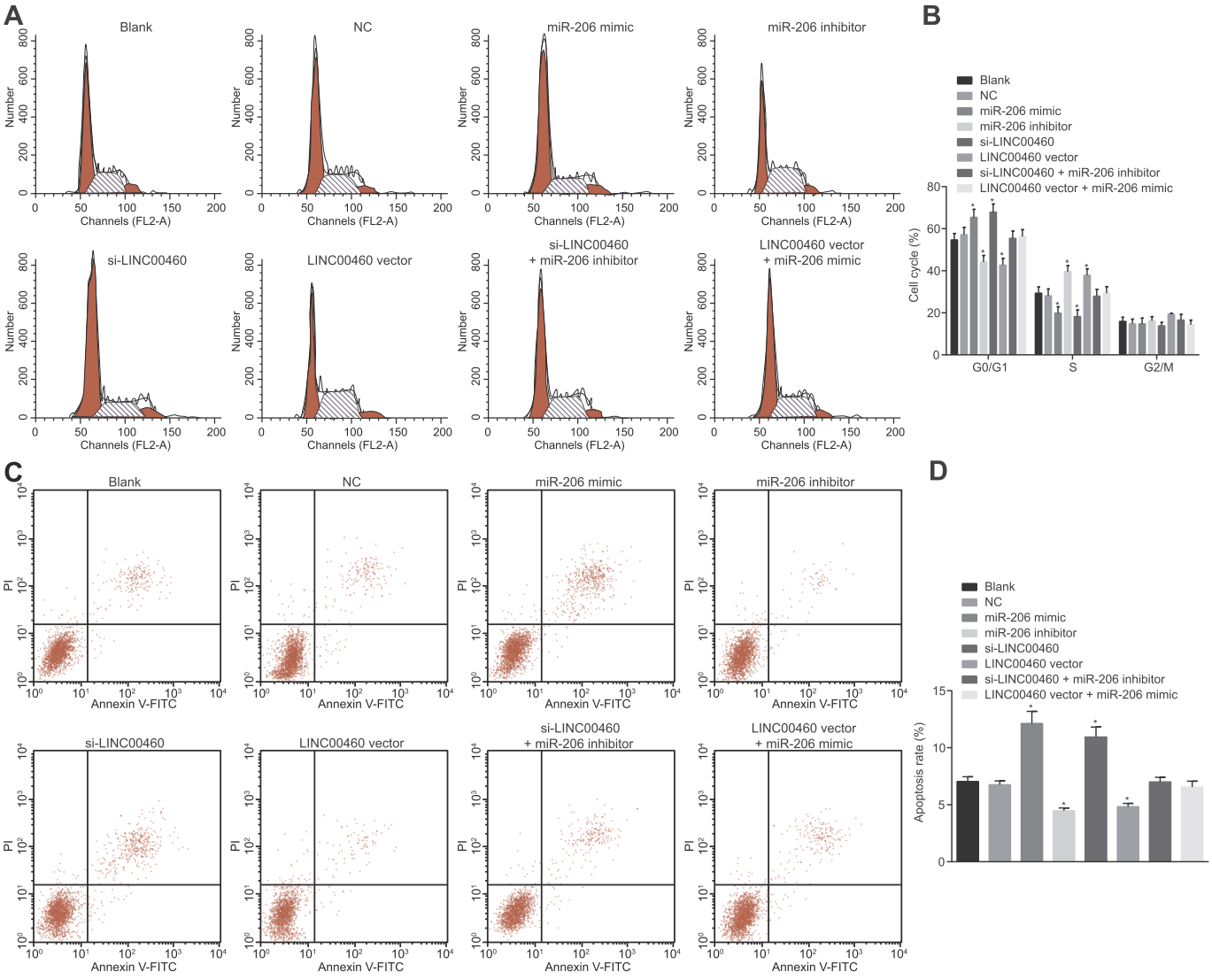

Fig. 6. Low expression of LINC00460 affects cell cycle distribution and promotes the apoptosis of HNSCC by sponging miR-206. A, cell cycle distribution of each group by PI staining. B, percentage of cell at different cell cycle of each group. C, apoptosis of cells in each group by Annexin V/PI double staining. D, percentage of apoptotic cells in each group. * $p < 0.05$ *vs.* the blank group and the NC group. All data in PI staining and Annexin V/PI double staining were expressed by mean ± standard deviation of three independent biological replicates, two-way ANOVA for percentage of cell cycle distribution, and one-way ANOVA for apoptosis of cells. HNSCC, head and neck squamous cell carcinoma; PI, propidium iodide; NC, negative control; ANOVA, analysis of variance.

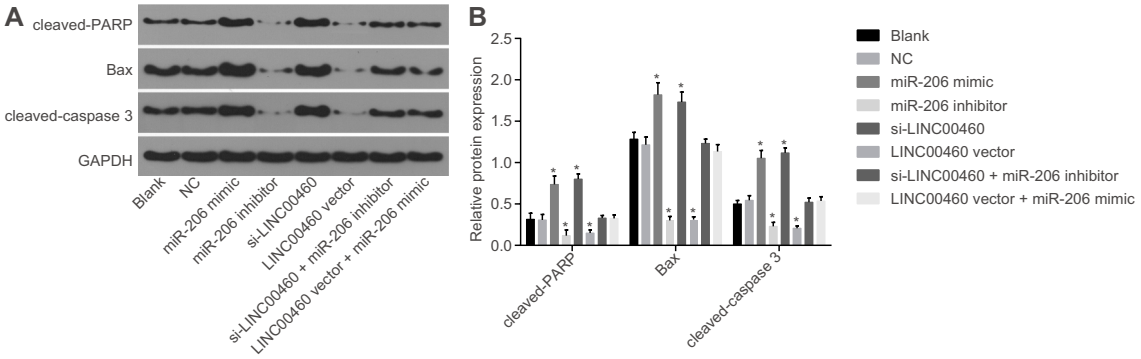

Fig. 7. Over-expression of miR-206 or silencing of LINC00460 promotes apoptosis of HNSCC cells. A. protein bands of cleaved-PARP, Bax and cleaved-caspase 3 and GAPDH. B, protein expression of cleaved-PARP, Bax and cleaved-caspase 3 in each group. * $p < 0.05$ *vs.* the blank group and the NC group. The data were expressed by mean ± standard deviation of three independent biological replicates, which were analyzed by one-way ANOVA. miR-206, microRNA-206; HNSCC, head and neck squamous cell carcinoma; Bax, Bcl-2-associated X protein; GAPDH, glyceraldehyde-3-phosphate dehydrogenase; NC, negative control; ANOVA, analysis of variance.

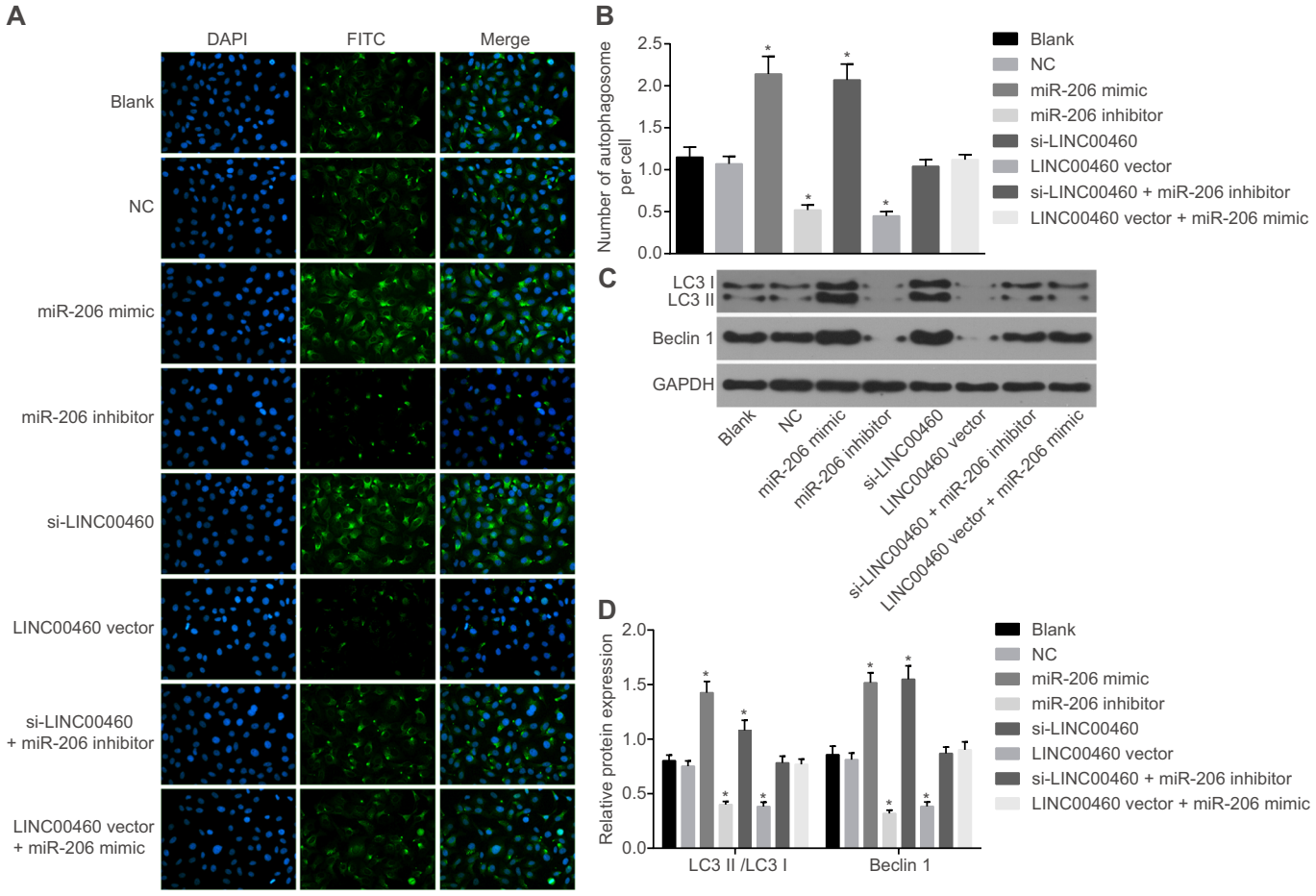

Fig. 8. High expression of miR-206 or low expression of LINC00460 promotes the autophagy of HNSCC cells. A, representative images of transfected cells examined by immunofluorescence assay. B, the amount of autophagosomes in each group. C, the protein bands of LC3 II, LC3 I, Beclin1 and GAPDH in each group. D, the protein expression of LC3 II, LC3 I and Beclin 1. All data were expressed as mean ± standard deviation of three independent biological replicates, which was analyzed by one-way ANOVA. * $p < 0.05$ *vs.* the blank group and the NC group. HNSCC, head and neck squamous cell carcinoma; ANOVA, analysis of variance; GAPDH, glyceraldehyde-3-phosphate dehydrogenase; NC, negative control.

projected an inferior 5-year survival rate than those who had a lower STC2 expression [11]. Accumulating evidence has demonstrated that STC2 was upregulated in various types of human cancers, including colorectal cancer and prostate cancer [12,13], which is in accordance with the results of our study. Through subsequent experiment, it was evident that the expressions of LINC00460, miR-206 and STC2 were closely correlated to TNM staging and differentiation degree of HNSCC. In accordance with our study, Y. Kita et al. highlighted that the STC2 expression was highly correlated with multiple clinicopathologic variables, such as poor cancer prognosis, tumor proliferation and lymphatic invasion predominantly through lymph node metastases [11]. Besides, Hu et al. revealed the highly dynamic and cell-specific patterns of lncRNAs during T cell development and differentiation, and the transcripts by mammalian genomes encoding thousands of lncRNAs played key roles in gene regulation and affected vital biological processes in cancer development and pathological conditions [22]. Apart from the above two factors, Zheng et al. discovered that an up-regulated expression of a certain type of miRNA-miR-15 was correlated not only with the advanced clinical TNM stage, but also with lymph node metastasis [23].

In addition, our results indicated that the upregulation of miR-206 and downregulation of LINC00460 stimulated the apoptosis and autophagy of HNSCC cells. The findings of a study by Xiao et al. reported that autophagy was regulated by a combination of multiple autophagy-related genes, such as LC3, which was located on the autophagosome membrane and essential for autophagosome formation [24]. An existing study also contributed to the speculation that numerous miRNAs regulate cell apoptosis, and it would be beneficial to inhibit autophagy and apoptosis conjointly [25]. miR-206 has been reported to exert its tumor suppressive properties in several cancers. For instance, it was revealed that miR-206 was poorly expressed in colorectal cancer (CRC), while the overexpression of miR-206 suppressed proliferation and also improved apoptosis by targeting TM4SF1 in CRC [26]. Poorly expressed miR-206 has also been found in cervical cancer (CC), and up-regulation of miR-206 led to an inhibited cell proliferation [27]. Additionally, LINC00460 was highly expressed in gastric cancer (GC) and CRC with unfavorable prognosis, suggesting that LINC00460 knockdown could inhibit the progression of CRC [28,29]. Furthermore, the relationships between LINC00460, STC2 and miR-206 were verified by means of dual luciferase reporter gene assay and RNA pull-down assay. The results also showed that upregulated miR-206 and downregulated LINC00460 decrease the mRNA and protein expression of STC2, which led to the conclusion that LINC00460 acted as a sponge to silence the miR-206 expression, and increase the expression of STC2 through impairing miR-206-targeted inhibition. Previous study suggested that miR-126 up-regulation reduced the ratio of phosphorylated AKT/ERK, indicating that miR-126 might be an important regulator in AKT/ERK signaling pathway [30], which is consistent with our finding that over-expressed miR-206 or silenced LINC00460 inhibits the AKT signaling pathway.

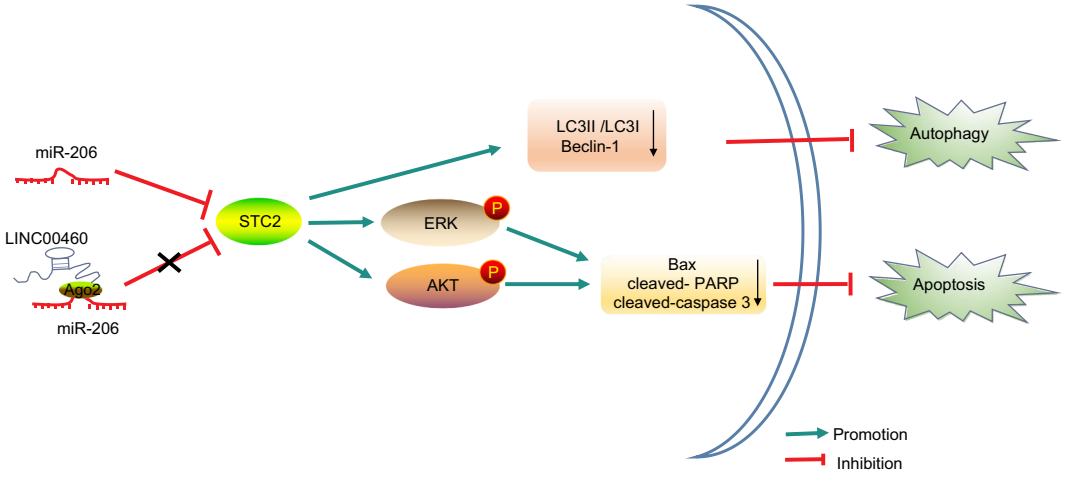

Fig. 9. The mechanism investigation demonstrated that upregulation of miR-206 or downregulation of LINC00460 promoted the apoptosis and autophagy of HNSCC cells. On one hand, upregulated STC2 inhibited autophagy by downregulating LC3 II/LC3 I ratio and Beclin-1 (autophagy related genes). On the other hand, upregulated STC2 inhibited the expression of cleaved-PARP, Bax and cleaved-caspase 3 proteins by activating ERK and AKT signaling pathways, and ultimately inhibits cell apoptosis. miR-206, microRNA-206; HNSCC, head and neck squamous cell carcinoma; STC2, Stanniocalcin-2; Bax, Bcl-2-associated X protein; AKT, Protein kinase B.

5. Conclusion

In conclusion, we have confirmed that LINC00460 and STC2 were highly expressed, while miR-206 was poorly expressed in HNSCC. We also demonstrated that the up-regulation of miR-206 or down-regulation of LINC00460 promoted the apoptosis and autophagy of HNSCC cells (Fig. 9). We surely speculated that LINC00460 silencing might be a promising target for HNSCC. However, only *in vitro* experiment was conducted in our study, which might cause biases in our results. A further in-depth study principally concentrating on the *in vitro* functions in more HNSCC cell lines as well as *in vivo* functions might increase the credibility of our results. Anyway, it should be noted that the LINC00460/STC2/miR-206 regulatory axis was crucial for affecting the development and progression of HNSCC and also provided theoretical basis for exploring the therapies for HNSCC.

Funding

None.

Acknowledgments

The authors would like to acknowledge the helpful comments on this paper received from the reviewers.

Conflicts of interest

The authors declare no conflicts of interest.

Author's contribution

Kai Xue designed the study. Jinqiu Li and Shanji Nan collated the data, carried out data analyses and produced the initial draft of the manuscript. Xue Zhao and Chengbi Xu contributed to drafting and polishing the manuscript. All authors have read and approved the final submitted manuscript.

References

[1] G. Childs, M. Fazzari, G. Kung, N. Kawachi, M. Brandwein-Gensler, M. McLemore, Q. Chen, R.D. Burk, R.V. Smith, M.B. Prystowsky, T.J. Belbin, N.F. Schlecht, Low-level expression of microRNAs let-7d and miR-205 are prognostic markers of head and neck squamous cell carcinoma, Am. J. Pathol. 174 (2009) 736–745.

[2] S. Yang, Q. Ji, B. Chang, Y. Wang, Y. Zhu, D. Li, C. Huang, Y. Wang, G. Sun, L. Zhang, Q. Guan, J. Xiang, W. Wei, Z. Lu, T. Liao, J. Meng, Z. Wang, B. Ma, L. Zhou, Y. Wang, G. Yang, STC2 promotes head and neck squamous cell carcinoma metastasis through modulating the PI3K/AKT/Snail signaling, Oncotarget 8 (2017) 5976–5991.

[3] W. Chen, R. Zheng, P.D. Baade, S. Zhang, H. Zeng, F. Bray, A. Jemal, X.Q. Yu, J. He, Cancer statistics in China, 2015, CA Cancer J. Clin. 66 (2016) 115–132.

[4] W. Cao, J.N. Liu, Z. Liu, X. Wang, Z.G. Han, T. Ji, W.T. Chen, X. Zou, A three-lncRNA signature derived from the Atlas of ncRNA in cancer (TANRIC) database predicts the survival of patients with head and neck squamous cell carcinoma, Oral Oncol. 65 (2017) 94–101.

[5] Campbell JD, Yau C, Bowlby R, Liu Y, Brennan K, Fan H, Taylor AM, Wang C, Walter V, Akbani R, Byers LA, Creighton CJ, Coarfa C, Shih J, Cherniack AD, Gevaert O, Prunello M, Shen H, Anur P, Chen J, Cheng H, Hayes DN, Bullman S, Pedamallu CS, Ojesina AI, Sadeghi S, Mungall KL, Robertson AG, Benz C, Schultz A, Kanchi RS, Gay CM, Hegde A, Diao L, Wang J, Ma W, Sumazin P, Chiu HS, Chen TW, Gunaratne P, Donehower L, Rader JS, Zuna R, Al-Ahmadie H, Lazar AJ, Flores ER, Tsai KY, Zhou JH, Rustgi AK, Drill E, Shen R, Wong CK, Cancer Genome Atlas Research N, Stuart JM, Laird PW, Hoadley KA, Weinstein JN, Peto M, Pickering CR, Chen Z, Van Waes C. Genomic, pathway network, and immunologic features distinguishing squamous carcinomas. Cell Rep. 23 (2018) 194–212 e196.

[6] J.R. Prensner, A.M. Chinnaiyan, The emergence of lncRNAs in cancer biology, Cancer Discov 1 (2011) 391–407.

[7] Y. Liang, Y. Wu, X. Chen, S. Zhang, K. Wang, X. Guan, K. Yang, J. Li, Y. Bai, A novel long noncoding RNA linc00460 up-regulated by CBP/P300 promotes carcinogenesis in esophageal squamous cell carcinoma, Biosci. Rep. 37 (2017).

[8] G. Chen, Z. Wang, D. Wang, C. Qiu, M. Liu, X. Chen, Q. Zhang, G. Yan, Q. Cui, LncRNADisease: a database for long-non-coding RNA-associated diseases, Nucleic Acids Res. 41 (2013) D983–D986.

[9] Q.Y. Yue, Y. Zhang, Effects of Linc00460 on cell migration and invasion through regulating epithelial-mesenchymal transition (EMT) in non-small cell lung cancer, Eur. Rev. Med. Pharmacol. Sci. 22 (2018) 1003–1010.

[10] O.M. Wilkins, A.J. Titus, J. Gui, M. Eliot, R.A. Butler, E.M. Sturgis, G. Li, K.T. Kelsey, B.C. Christensen, Genome-scale identification of microRNA-related SNPs associated with risk of head and neck squamous cell carcinoma, Carcinogenesis 38 (2017) 986–993.

[11] Y. Kita, K. Mimori, M. Iwatsuki, T. Yokobori, K. Ieta, F. Tanaka, H. Ishii, H. Okumura, S. Natsugoe, M. Mori, STC2: a predictive marker for lymph node metastasis in esophageal squamous-cell carcinoma, Ann. Surg. Oncol. 18 (2011) 261–272.

[12] K. Ieta, F. Tanaka, T. Yokobori, Y. Kita, N. Haraguchi, K. Mimori, H. Kato, T. Asao, H. Inoue, H. Kuwano, M. Mori, Clinicopathological significance of stanniocalcin 2 gene expression in colorectal cancer, Int. J. Cancer 125 (2009) 926–931.

[13] K. Tamura, M. Furihata, S.Y. Chung, M. Uemura, H. Yoshioka, T. Iiyama, S. Ashida, Y. Nasu, T. Fujioka, T. Shuin, Y. Nakamura, H. Nakagawa, Stanniocalcin 2 overexpression in castration-resistant prostate cancer and aggressive prostate cancer, Cancer Sci. 100 (2009) 914–919.

[14] M.D. Robinson, D.J. McCarthy, G.K. Smyth, edgeR: a Bioconductor package for differential expression analysis of digital gene expression data, Bioinformatics 26 (2010) 139–140.

[15] F. Bohrnsen, M. Fricke, C. Sander, A. Leha, H. Schliephake, F.J. Kramer, Interactions of human MSC with head and neck squamous cell carcinoma cell line PCI-13 reduce markers of epithelia-mesenchymal transition, Clin. Oral Investig. 19 (2015)

1121–1128.
[16] M. Zhao, D. Sano, C.R. Pickering, S.A. Jasser, Y.C. Henderson, G.L. Clayman, E.M. Sturgis, T.J. Ow, R. Lotan, T.E. Carey, P.G. Sacks, J.R. Grandis, D. Sidransky, N.E. Heldin, J.N. Myers, Assembly and initial characterization of a panel of 85 genomically validated cell lines from diverse head and neck tumor sites, Clin. Cancer Res. 17 (2011) 7248–7264.
[17] M. Yu, S.K. Selvaraj, M.M. Liang-Chu, S. Aghajani, M. Busse, J. Yuan, G. Lee, F. Peale, C. Klijn, R. Bourgon, J.S. Kaminker, R.M. Neve, A resource for cell line authentication, annotation and quality control, Nature 520 (2015) 307–311.
[18] J.C. Brenner, M.P. Graham, B. Kumar, L.M. Saunders, R. Kupfer, R.H. Lyons, C.R. Bradford, T.E. Carey, Genotyping of 73 UM-SCC head and neck squamous cell carcinoma cell lines, Head Neck 32 (2010) 417–426.
[19] N. Stransky, A.M. Egloff, A.D. Tward, A.D. Kostic, K. Cibulskis, A. Sivachenko, G.V. Kryukov, M.S. Lawrence, C. Sougnez, A. McKenna, E. Shefler, A.H. Ramos, P. Stojanov, S.L. Carter, D. Voet, M.L. Cortes, D. Auclair, M.F. Berger, G. Saksena, C. Guiducci, R.C. Onofrio, M. Parkin, M. Romkes, J.L. Weissfeld, R.R. Seethala, L. Wang, C. Rangel-Escareno, J.C. Fernandez-Lopez, A. Hidalgo-Miranda, J. Melendez-Zajgla, W. Winckler, K. Ardlie, S.B. Gabriel, M. Meyerson, E.S. Lander, G. Getz, T.R. Golub, L.A. Garraway, J.R. Grandis, The mutational landscape of head and neck squamous cell carcinoma, Science 333 (2011) 1157–1160.
[20] Y.G. Kong, M. Cui, S.M. Chen, Y. Xu, Y. Xu, Z.Z. Tao, LncRNA-LINC00460 facilitates nasopharyngeal carcinoma tumorigenesis through sponging miR-149-5p to up-regulate IL6, Gene 639 (2018) 77–84.
[21] T. Zhang, M. Liu, C. Wang, C. Lin, Y. Sun, D. Jin, Down-regulation of MiR-206 promotes proliferation and invasion of laryngeal cancer by regulating VEGF expression, Anticancer Res. 31 (2011) 3859–3863.
[22] G. Hu, Q. Tang, S. Sharma, F. Yu, T.M. Escobar, S.A. Muljo, J. Zhu, K. Zhao, Expression and regulation of intergenic long noncoding RNAs during T cell development and differentiation, Nat. Immunol. 14 (2013) 1190–1198.
[23] S.R. Zheng, G.L. Guo, W. Zhang, G.L. Huang, X.Q. Hu, J. Zhu, Q.D. Huang, J. You, X.H. Zhang, Clinical significance of miR-155 expression in breast cancer and effects of miR-155 ASO on cell viability and apoptosis, Oncol. Rep. 27 (2012) 1149–1155.
[24] Y. Kabeya, N. Mizushima, T. Ueno, A. Yamamoto, T. Kirisako, T. Noda, E. Kominami, Y. Ohsumi, T. Yoshimori, LC3, a mammalian homologue of yeast Apg8p, is localized in autophagosome membranes after processing, EMBO J. 19 (2000) 5720–5728.
[25] J. Xiao, X. Zhu, B. He, Y. Zhang, B. Kang, Z. Wang, X. Ni, MiR-204 regulates cardiomyocyte autophagy induced by ischemia-reperfusion through LC3-II, J. Biomed. Sci. 18 (2011) 35.
[26] Y.R. Park, S.Y. Seo, S.L. Kim, S.M. Zhu, S. Chun, J.M. Oh, M.R. Lee, S.H. Kim, I.H. Kim, S.O. Lee, S.T. Lee, S.W. Kim, MiRNA-206 suppresses PGE2-induced colorectal cancer cell proliferation, migration, and invasion by targetting TM4SF1, Biosci. Rep. 38 (2018).
[27] J. Cui, Y. Pan, J. Wang, Y. Liu, H. Wang, H. Li, MicroRNA-206 suppresses proliferation and predicts poor prognosis of HR-HPV-positive cervical cancer cells by targeting G6PD, Oncol. Lett. 16 (2018) 5946–5952.
[28] F. Wang, S. Liang, X. Liu, L. Han, J. Wang, Q. Du, LINC00460 modulates KDM2A to promote cell proliferation and migration by targeting miR-342-3p in gastric cancer, Onco Targets Ther 11 (2018) 6383–6394.
[29] Y. Lian, C. Yan, H. Xu, J. Yang, Y. Yu, J. Zhou, Y. Shi, J. Ren, G. Ji, K. Wang, A novel lncRNA, LINC00460, affects cell proliferation and apoptosis by regulating KLF2 and CUL4A expression in colorectal Cancer, Mol Ther Nucleic Acids 12 (2018) 684–697.
[30] Y. Liu, Y. Zhou, X. Feng, P. An, X. Quan, H. Wang, S. Ye, C. Yu, Y. He, H. Luo, MicroRNA-126 functions as a tumor suppressor in colorectal cancer cells by targeting CXCR4 via the AKT and ERK1/2 signaling pathways, Int. J. Oncol. 44 (2014) 203–210.